TOTAL INTERNAL REFLECTION FLUORESCENCE MICROSCOPY (TIRFM) OF ACRIDINE ORANGE IN SINGLE CELLS

REINHARD SAILER[1], KARL STOCK[1,2], WOLFGANG S.L. STRAUSS[1], MARCO LYTTEK[2], AND HERBERT SCHNECKENBURGER[1,2,*]

[1]Institut für Lasertechnologien in der Medizin und Messtechnik an der Universität Ulm, Helmholtzstr. 12, 89081 Ulm, Germany;

[2]Fachhochschule Aalen, Institut für Angewandte Forschung, 73428 Aalen, Germany

* Corresponding author, Tel. +49-7361-568229, FAX +49-7361-568225, e-mail: herbert.schneckenburger@fh-aalen.de

Key Words: endothelial cells, cell organelles, fluorescence microscopy, TIRFM

Summary: A miniaturized condensor unit for variable-angle total internal reflection fluorescence microscopy (TIRFM) has been developed and used for studies of cultivated endothelial cells incubated with the organelle marker acridine orange (AO). Upon excitation by an evanescent electromagnetic field, the penetration depth of incident light could be varied between about 50 nm and more than 200 nm. TIRFM signals were compared with fluorescence from the whole cell. AO fluorescence arising from the cell nucleus, lysosomes and those parts of the cytoplasm which were in close proximity to the plasma membrane, were thus distinguished. The selectivity of the method was further improved by using spectral and temporal (nanosecond) resolution.

INTRODUCTION

High lateral and axial resolution are challenges in fluorescence microscopy. Using high aperture lenses and contrast-enhanced detection, a lateral resolution around 200 nm and an axial resolution around 500 nm can be attained. Object diameters, however, are often larger, and clear images from the focal plane are superimposed by out-of-focus fluorescence images from adjacent parts of the sample. In the past years this disadvantage has heen overcome by laser scanning microscopy with the object being located precisely in the focus of the illuminating laser beam. A pinhole within the image plane or a two-photon excitation technique permit selective detection from this focal plane. Microscopic images are obtained by horizontal scanning of the laser beam; 3-dimensional information is achieved by moving the sample in vertical direction. Axial resolution, however, remains in the range of some hundreds of nanometers and is therefore considerably larger than the

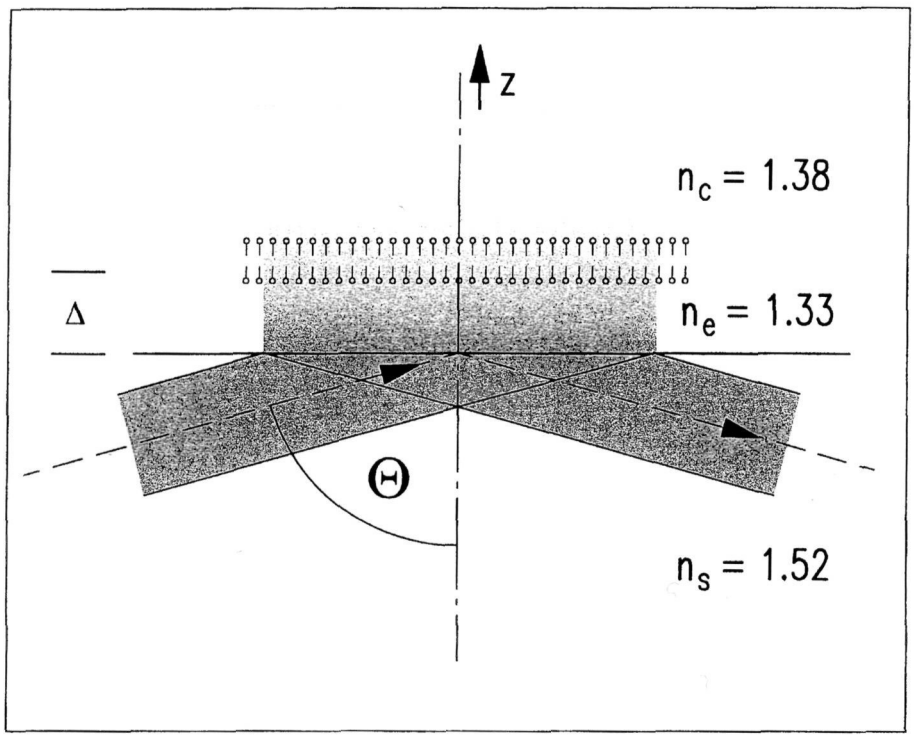

Fig. 1: Total internal reflection and evanescent electromagnetic field. The refractive indices of the substrate (n_s), extracellular medium (n_e) and cytoplasm (n_c) as well as the average distance between the reflecting surface and the plasma membrane (Δ) are indicated.

diameters of cell membranes or many organelles. For this reason, *Total internal reflection fluorescence microscopy* (TIRFM) has been established in order to study the plasma membrane and adjacent cellular sites with an improved axial resolution,

TIRFM techniques utilize an evanescent electromagnetic field for the excitation of fluorophores. This field arises upon total reflection of the excitation light at the cell-substrate interface, when the angle of incidence Θ is larger than the critical angle $\Theta_C = \arcsin n_c/n_s$, with n_c and n_s being the refractive indices of the cytoplasm and the cell substrate (e.g. glass slide), respectively. Fig. 1 shows the totally reflected light beam as well as the evanescent field, whose intensity decays exponentially with the distance ζ from the cell-substrate interface. Its penetration depth depends on the wavelength and the incident angle of the excitation light as well as on n_c and n_s. Typically, penetration depths can be varied between 50 and more than 200 nm (Burmeister et al. 1994) thus permitting selective excitation of fluorophores located in or close to the plasma membrane. So far, TIRFM has been applied for studies of the topography of cell-substrate contacts (Axelrod 1981, Truskey et al. 1992, Hornung et al. 1996), for measuring diffusion and self-associ-

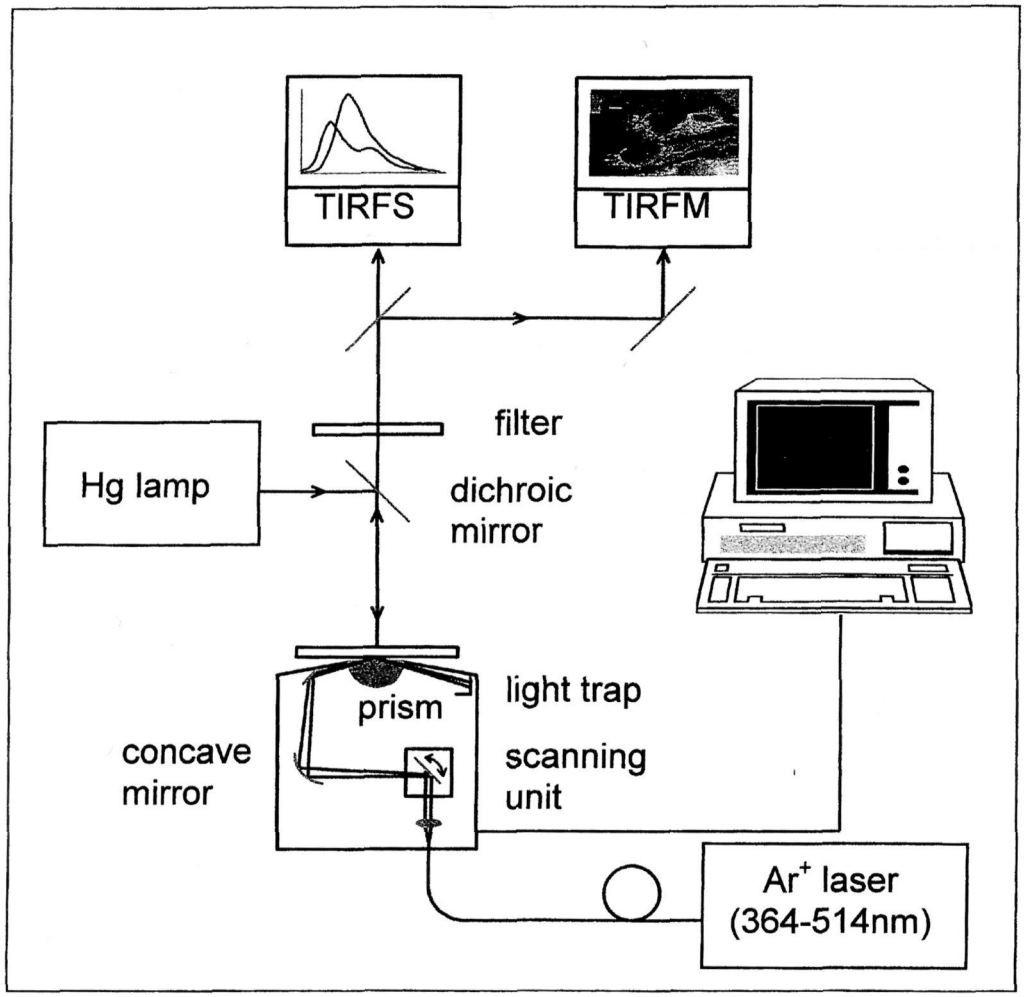

Fig. 2: Experimental setup of variable-angle total internal reflection fluorescence spectroscopy (TIRFS) and microscopy (TIRFM).

ation of proteins in membranes (Thompson et al. 1997), for detection of membrane-proximal ion fluxes (Omann and Axelrod 1996), for studies of photosensitizers in close proximity to plasma membranes (Strauss et al. 1998, Sailer et al. 2000), as well as for imaging of endocytosis or exocytosis (Betz et al. 1996, Oheim et al. 1998). In addition, by variation of the angle of incidence, fluorophores can be even more precisely localized within the cytoplasm, the plama membrane (Stock et al. 1999) or spherically-shaped organelles such as lysosomes (Oheim et al. 1998). In the present article a novel device of variable-angle TIRFM and preliminary applications to the fluorescence marker acridine orange (AO) are described. AO is well-known for staining cell nuclei as well as lysosomes, showing green fluorescence at low concentration (~ 10^{-7} M) and orange fluorescence at rather high concentration (Allison and Young 1964). This red shift has been related to dimerization or oligomerization of AO molecules.

MATERIALS AND METHODS

BKEz-7 endothelial cells from the calf aorta (Halle et al. 1984) were routinely grown on microscope object slides in Eagle's minimum essential medium (MEM) supplemented with 10% fetal calf serum (FCS), glutamine (4mM) and antibiotics (penicillin, streptomycin) at 37°C and 5% CO_2. Subconfluently growing cell monolayers were obtained 48 h after seeding of 150 cells/mm^2 on microscope object slides. After this period cells were incubated for 30 min. with 5 μM AO dissolved within the culture medium and rinsed twice with AO-free medium prior to TIRFM measurements.

For TIRFM measurements a conventional fluorescence microscope (Axioplan, Carl Zeiss Jena) was equipped with an integrating CCD camera (DMX-950P, Sony, 752 x 582 Pixels) for image detection as well as with a custom-made polychromator, an image intensifier and an optical multichannel analyzer (IMD C4562, Hamamatsu Photonics) for fluorescence spectroscopy (Schneckenburger et al. 1998). The image intensifier could be operated in a continuous wave (cw) as well as in a time-gated mode for detection of emission spectra within time windows of 5 ns, which could be shifted with reference to pulsed laser excitation. In order to vary the angle of incidence Θ, a miniaturized microscope condensor unit was developed. This condensor unit consists of a hemicylindrical glass prism optically coupled to the object slide, an adjustable mirror and focusing optics. An image from the adjustable mirror is created on the sample, which is located in the centre of the hemicylinder. When rotating the mirror by a step motor, identical parts of the sample can be illuminated at different angles Θ. This permits variation of the penetration depth of the evanescent field and allows for axial resolution of fluorescence in the nanometer range. Light of an argon ion laser (Innova 90, Coherent, λ = 364-514 nm) is coupled to the condensor unit by monomode fiber. This laser can also be used in combination with an acousto-optic modulator and a pulse picker for time-resolved fluorescence microscopy in the nanosecond range. Alternatively, a pulsed Nd:YAG laser (DCR 11, Spectra Physics, λ = 355 nm, pulse duration 2 ns, repetition rate 10 Hz) and an optical parametric oscillator (BBO 355-vis; Opta GmbH) for wavelength tunig between 410 and 680 nm were used as excitation sources. The incident light was always polarized such that its electric field vector was perpendicular to the plane of incidence. A scheme of the whole setup is shown in Fig. 2. In addition to TIRFM, fluorescence of the samples could also be excited by epiillumination using a high pressure mercury lamp together with a dichroic mirror and appropriate optical filters.

RESULTS AND DISCUSSION

Fluorescence images of BKEz-7 endothelial cells incubated with AO using epiillumination in a wavelength range of 450-490 nm (a) or TIR illumination at an excitation wavelength of 488 nm and angles of incidence Θ = 66° (b), 68° (c) or 70° (d) are shown in Fig. 3. Since for refractive indices n_c = 1.37 and n_s = 1.515 the critical angle of total internal reflection is 64.7°, penetration depths of the ex-

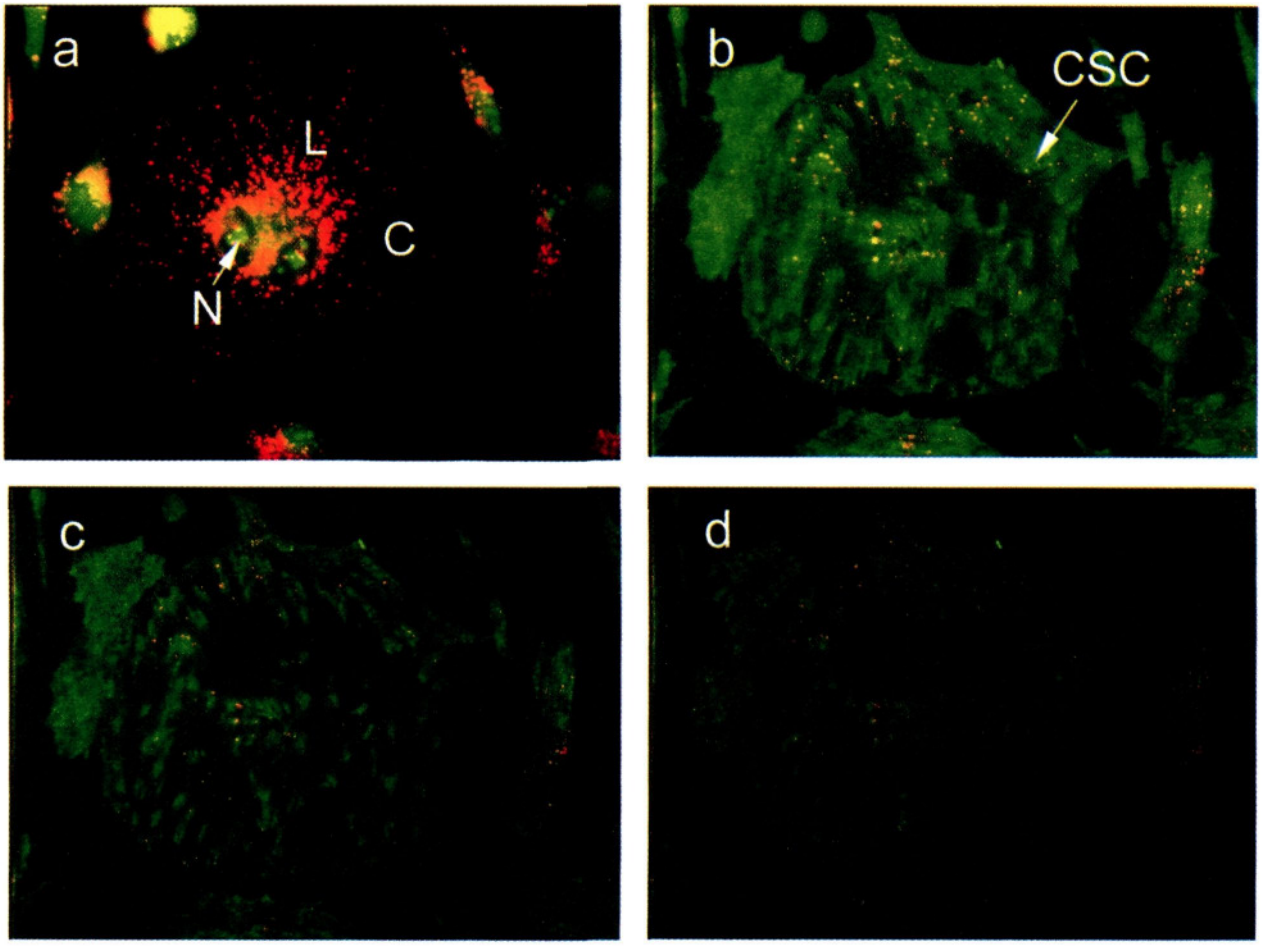

Fig. 3: Fluorescence images of BKEz-7 endothelial cells incubated with acridine orange (5 µM; 30 min.): epiilluminaiton at λ = 450-490 nm (a); TIR illumination at Θ = 66° (b), 68° (c) and 70°(d); fluorescence detected at $\lambda > 510$ nm; image size 160x110 µm^2 (L = lysosomes; C = cytoplasm; N = nucleolus; CSC = cell-substrate contact).

citation light at $\Theta \geq 66°$ are below 200 nm. When using illumination of whole cells (a), fluorescence arises from well defined organelles, i.e. lysosomes (L) and nucleoli (N) as well as (more diffusely) from the cytoplasm (C). The fluorescence from the cell nucleus and the cytoplasm appears green, whereas the luminescence from lysosomes appears in orange colour. These different emission wavelengths reflect lower AO concentrations within the nucleus as well as within the cytoplasm and higher AO concentrations within lysosomes. When using an angle of incidence $\Theta \geq 66°$ (b-d), mainly green fluorescence from those parts of the cytoplasm is measured, which are close to the plasma membrane. At 66° a few lysosomes in close proximity to the plasma membrane are still resolved, whereas at larger angles only AO fluorescence from the cytoplasm is detected. Its intensity decreases with increasing angle Θ corresponding to a decreasing penetration depth and intensity of the evanescent field. The inhomogenous fluorescence pattern reflects the vari-

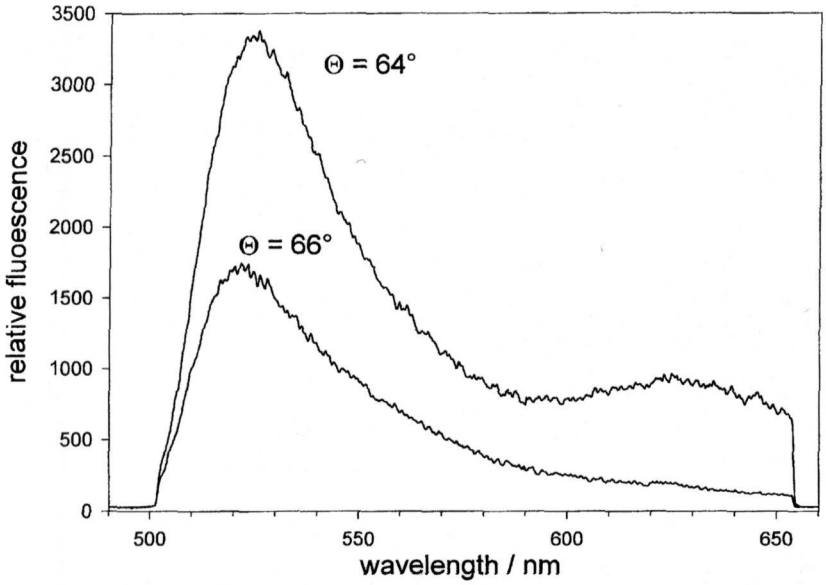

Fig. 4: Fluorescence spectra of BKEz-7 endothelial cells incubated with acridine orange; (5µM, 30 min.). Excitation at λ = 488 nm and Θ = 64° (total cell) or 66° (TIR).

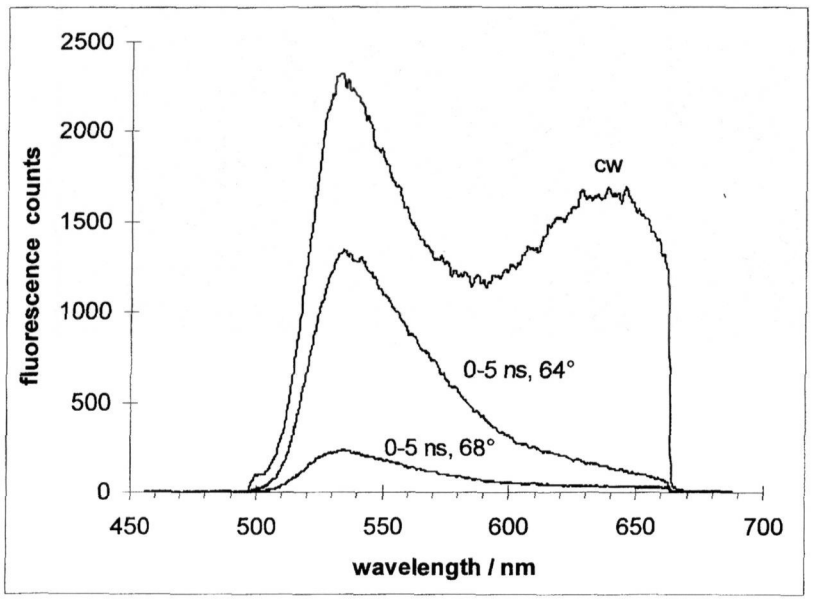

Fig. 5: Fluorescence spectra of BKEz-7 endothelial cells incubated with acridine orange; (5µM, 30 min). Cw epiillumination at λ = 450-490 nm (upper curve) and time-gated TIR illumination at Θ = 64° (total cell) or 68° (TIR).

able distance between the plasma membrane and the glass substrate, which only in so-called focal contacts is close to 0. Corresponding fluorescence spectra for Θ = 64° and Θ = 66° are shown in Fig. 4. In comparison with illumination of whole cells (Θ = 64°) the intensity of the green fluorescent band centered around 525 nm decreases, whereas the orange band (maximum around 625 nm) disappears completely under TIRFM conditions (Θ = 66°). This again shows that no or very few lysosomes are located in close proximity to the plasma membrane.

Separation of lysosomal and cytoplasmic AO fluorescence is further improved when cells are illuminated by short laser pulses, and when their emission is measured within nanosecond time gates with variable delay time after laser excitation. Fluorescence decay times of about 4 ns and 15 ns were measured at λ = 505-550 nm and λ ≥ 590 nm, respectively. Similar lifetimes were previously reported for AO monomers and dimers in aequeous and premicellar solutions (Miyoshi et al.

1988). A more detailed analysis of fluorescence decay kinetics shows that the shorter time constant may result from two components with lifetimes of 1.0 ns and 5.8 ns. In Fig. 5, fluorescence spectra of AO are depicted using the excitation band of 450-490 nm of the mercury lamp (upper curve) or the wavelength of 480 nm of the optical parametric oscillator (other curves). The upper curve, recorded at cw excitation of whole cells, shows pronounced emission bands of AO monomers and dimers around 525 nm and 630 nm, respectively. The other curves show emission spectra within time gates of 0-5 ns, i.e. during and immediately after the exciting laser pulse using angles of irradiation of 64° (whole cell illumination; middle curve) or 68° (TIR excitation; lower curve). In both cases, dimer fluorescence is considerably reduced due to its long lifetime. It appears as a weak shoulder at $\Theta = 64°$ and disappears completely at $\Theta = 68°$. At time gates of 5-10 ns or later the dimer band around 630 nm is clearly resolved at an irradiation angle of 64°, but remains negligible at $\Theta = 68°$.

CONCLUSION

Fluorescence from the plasma membrane and adjacent parts of the cytoplasm is measured selectively by TIRFM and distinguished from the emission of intracellular organelles. Selectivity is even enhanced when using spectral or temporal (nanosecond) resolution. By combination of TIRFM and time-resolved spectroscopy a phase transition of lipids in the plasma membrane has recently been proved using the membrane marker laurdan (Schneckenburger et al. 2000). The method appears also appropriate for detection of ion channels, protein channels or specific receptors in plasma membranes. Due to the low penetration depth of excitation light (around 50 nm) at large angles of incidence, the examined sample volume may become very small, and even detection of single fluorescent molecules appears possible.

Acknowledgments: The authors thank C. Hintze for technical assistance. Current research is supported by the Bundesministerium für Bildung und Forschung, grant no. 13N7514.

REFERENCES

Allison AC, Young MR, 1964. Uptake of dyes and drugs by living cells in culture. Life Sci 3: 1407-1414.

Axelrod D, 1981. Cell-substrate contacts illuminated by total internal reflection fluorescence. J Cell Biol 89: 141-145.

Betz WJ, Mao F, Smith CB, 1996. Imaging exocytosis and endocytosis. Curr Opin Neurobiol 6: 365-371.

Burmeister JS, Truskey GA, Reichert WM, 1994. Quantitative analysis of variable-angle total internal reflection fluorescence microscopy (VA-TIRFM) of cell / substrate contacts, J Microsc 173: 39-51.

Halle W Siems W-E, Jentzsch KD, Teuscher E, Göres E, 1984. Die *in vitro* kultivierte Aorten-Endothelzelle in der Wirkstofforschung. Zellphysiologische Charakterisierung und Einsatzmöglichkeiten der Zellinie BKEz-7. Pharmazie 39:77-81.

Hornung J, Müller T, Fuhr G, 1996. Cryopreservation of anchorage-dependent mammalian cells fixed to structured glass and silicon substrates. Cryobiology 33: 260-270.

Miyoshi N, Hara K, Yokoyama I, Tomita G, Fukuda M, 1988. Fluorescence lifetime of acridine orange in sodium dodecyl sulfate premicellar solutions. Photochem Photobiol 47: 685-688.

Oheim M, Loerke D, Stühmer W, Chow RH, 1998. The last few milliseconds in the life of a secretory granule. Eur J Biophys 27: 83-98.

Omann GM, Axelrod D, 1996. Membrane-proximal calcium transients in stimulated neutrophils detected by total internal reflection fluorescence. Biophys J 71:2885-2891.

Sailer R, Strauss WSL, Emmert H, Stock K, Steiner R, Schneckenburger H, 2000. Plasma membrane associated location of sulfonated meso-tetraphenylporphyrins of different hydrophilicity probed by total internal reflection fluorescence spectroscopy. Photochem Photobiol 71: 460-465.

Schneckenburger H, Gschwend MH, Sailer R, Mock H-P, Strauss WSL, 1998. Time-gated fluorescence microscopy in molecular and cellular biology. Cell Mol Biol 44: 795-805.

Schneckenburger H, Stock K, Eickholz J, Strauss WSL, Lyttek M, Sailer R, 2000. Time-resolved total internal reflection fluorescence spectroscopy: application to the membrane marker laurdan. In: König K, Schneckenburger H, Tanke H (eds), Laser Microscopy. Proc SPIE, 4164: 36-42.

Stock K, Sailer R, Strauss WSL, Pavesi R, Lyttek M, Emmert H, Schneckenburger H, 1999. Total internal reflection fluorescence spectroscopy and microscopy (TIRFS/TIRFM) in cell biology and photobiology. In: Kotyk A (ed) Fluorescence Microscopy and Fluorescent Probes. Espero Publishing, Prague, Vol. 3: pp 67-79.

Strauss WSL, Sailer R, Gschwend MH, Emmert H, Steiner R, Schneckenburger H, 1998. Selective examination of plasma associated photosensitizers using total internal reflection fluorescence spectroscopy (TIRFS) - correlation between photobleaching and photodynamic efficacy of protoporphyrin IX. Photochem Photobiol 67: 363-369.

Thompson NL, Drake AW, Chen L, Broek WV, 1997. Equilibrium, kinetics, diffusion and self-association of proteins at membrane surfaces: Measurement by total internal reflection fluorescence microscopy. Photochem Photobio. 65: 39-46.

Truskey GA, Burmeister JS, Grapa E, Reichert WM, 1992. Total internal reflection fluorescence microscopy (TIRFM) (II) Topographical mapping of relative cell/substratum separation distances. J Cell Sci 103: 491-499.

Received: Nov. 13, 2000 Accepted: March 30, 2001